

Magnetic Errors of the LHC Dipoles and Possible Cures

R. Bartolini, P. Fessia, D. Perini, W. Scandale, E. Todesco
CERN, LHC Division, CH 1211 Geneva, Switzerland

Abstract

Nonlinear magnetic errors reduce the stable region of the particle motion thereby decreasing the performance of the collider. A careful analysis of the sources of magnetic field errors is mandatory and a statistical model of field imperfection is demanded to identify the causes that give rise to these errors and to implement corrective strategies already at the production level. Sorting strategies for the improvement of the dynamic aperture of the LHC are also discussed.

1 Introduction

The single particle beam dynamic in superconducting hadron colliders is dominated by nonlinear errors in the main magnets. Nonlinear fields induce instability in particle trajectories limiting the region of stable motion and thereby decreasing the accumulated intensity and the luminosity of the collider. This phenomenon is particularly harmful during the injection plateau, when the beam size is maximum.

There are three main sources of field imperfections in a superconducting magnet, namely, the non-ideal geometry of the coils, the persistent currents and the iron saturation. The iron saturation is almost irrelevant at the excitation level of the injection plateau. The persistent currents, mostly determined by the size of the superconducting filament adopted, are estimated separately and their effect is eventually cancelled by an appropriate optimisation of the cross-section geometry. In the following sections, we will only concentrate our attention on the non-ideal shape of coils, and on the possible cure to reduce its effect in the LHC dipoles with two-in-one design.

The nominal shape of the coils already introduce significant systematic components in the magnetic field. In addition, the mechanical tolerances produce random deviations of multipolar harmonics from magnet to magnet. Coil deformations due to the assembly prestress or to the thermal shrinkage during the cool-down are also a potential source of field errors which must be known and possibly controlled.

The plane of this paper is the following. In Sections 2 and 3 we evaluate the magnetic errors induced in the LHC main dipoles by the geometrical imperfections of the coils. In Section 4 we suggest possible corrective actions based on the use of an appropriate set of shims during the assembly of the coils. In section 5 we suggest how we can reduce the effect of random errors by an appropriate sorting of the main dipoles during the installation and we present estimates of the possible improvement of beam stability. In Section 6 we draw some conclusions.

2 Systematic and random field-shape errors due to coil geometry

Let us consider the LHC dipole with the 5-block coil design shown in Fig.1. We expect to observe systematic field-shape errors even when the conductors are in their nominal position. The harmonic expected at injection are shown in Table 1. They result from an optimisation where the cross section of the coils is iteratively modified as to minimise or cancel the effect of persistent currents on the 'allowed' harmonics b_3 , b_5 , b_7 and b_9 . On the other hand, errors in coil positioning within mechanical tolerances generate field-shape imperfections randomly varying from dipole to dipole. To compute in a rough manner the field variation, we use a simplified and not fully consistent description of the coil displacement. We vary in an independent manner the radial and the azimuthal position of each block of superconducting cables with a Gaussian distribution with zero average and an appropriate value of the r.m.s. displacement. In

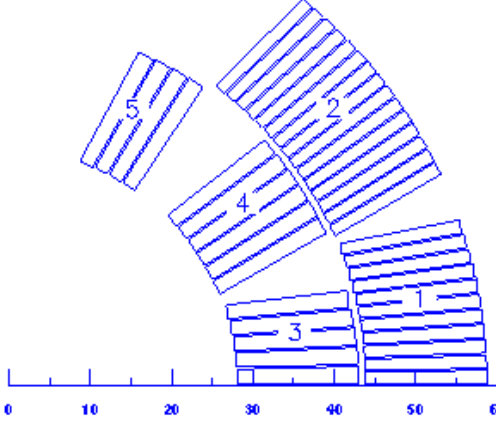


Fig. 1: Five blocks coil cross-section.

Table 1: Systematic errors expected at injection in the LHC dipoles. Unit 10^{-4} at the reference radius of 17 mm.

	nominal	geometric	pers. current
b_3	-11.76	0.29	-12.05
b_5	0.16	-1.59	1.75
b_7	0.53	0.83	-0.30
b_9	0.52	-0.70	0.18
b_{11}	1.77	1.77	-

Table 2 we present six columns. The first two give the random errors computed with ROXIE [1] assuming an r.m.s. displacement of the blocks of $50 \mu\text{m}$ and a distribution cut at 1σ . The corresponding distributions of the multipolar components are shown in Fig. 2. In the third and fourth columns of Table 2 we report the random multipolar errors extrapolated from the harmonics measured in the HERA dipoles and in the last two columns we show the estimated variations of the field errors expected from vendor to vendor [2]. Indeed, the results of our simple estimate of the random errors are consistent with the extrapolations from the results of Hera, except for high order components. This discrepancy is likely to be due to the limited precision of the magnetic measurement system rather than to a structural reason. The errors given in the last four columns of Table 2 are used in the computer tracking simulations of Section 5. They do not reduce in a dramatic manner the beam stability.

Looser mechanical tolerances generate larger random field errors: in Table 3 we show the random error obtained assuming r.m.s. displacements of $50 \mu\text{m}$ and of $100 \mu\text{m}$ and a distribution cut at 3σ .

Another source of magnetic errors varying from dipole to dipole is related to the imperfect shape of the collars. To estimate this effect in a proper manner we need a statistical model of the possible collar deformations, which is non yet available. We can however, evaluate the order of magnitude of the induced field imperfection by an 'ad hoc' model. We assume somehow arbitrarily that all the collars of a given dipole have the same shape with some deformation localised in a precise azimuthal sector of the cross-section. We also assume that the deviation is as large as the allowed mechanical tolerance.

Some of the magnetic errors induced by the considered modes of collar deformations are shown in dashed in Fig. 2. Our analysis is by far non-exhaustive. However, it is already sufficient to show that the magnetic errors due to collar tolerances have the same order of magnitude as the random errors of Table 2. It is interesting to note that for low order harmonics, i.e. below $n = 4$, the effect of the collar deformations seems to be the leading source of random errors; for high order harmonics, instead, this effect becomes smaller and smaller.

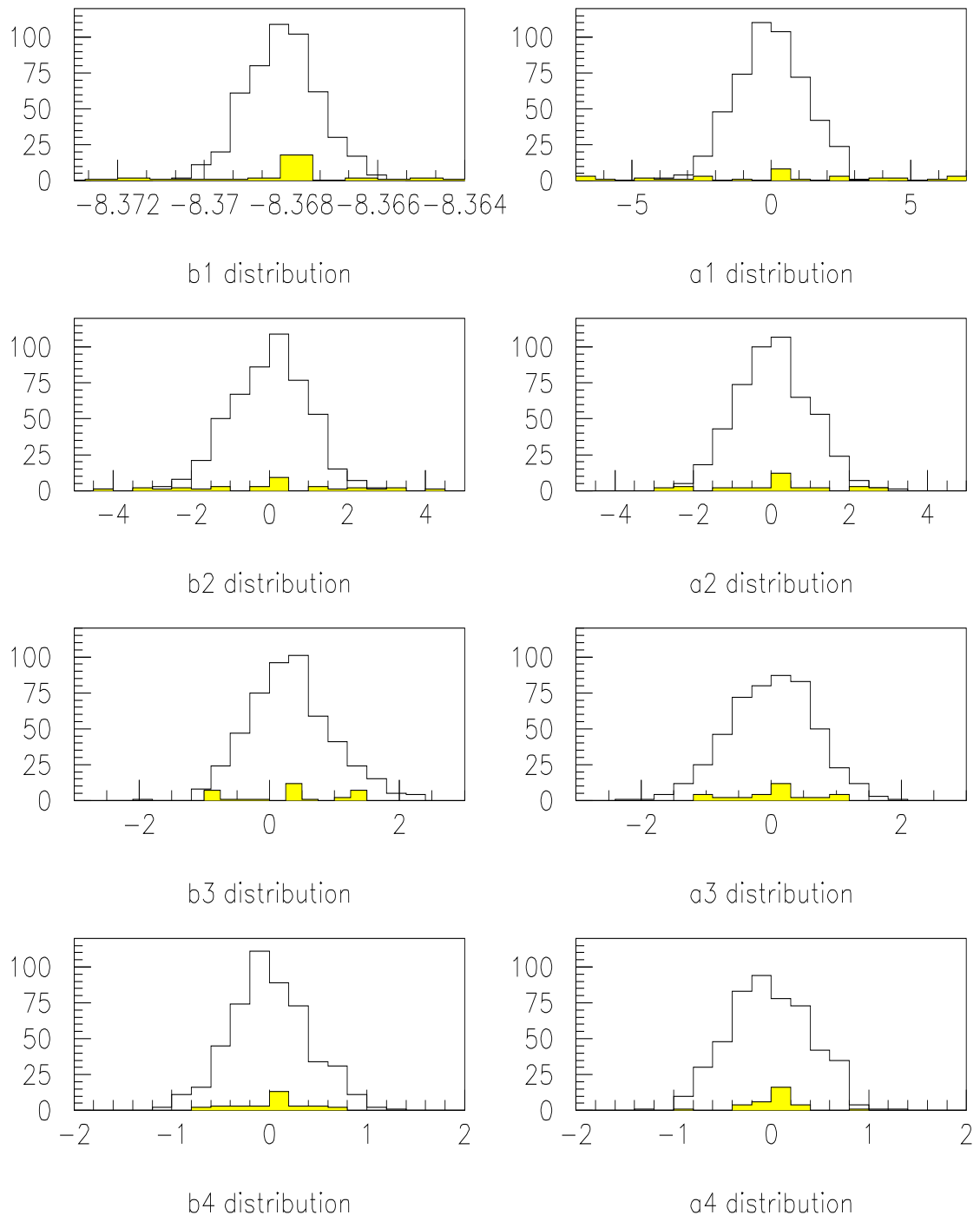


Fig. 2: Multipolar errors distribution for 500 realization of random blocks displacements (white background) and for maximal collar displacements (dark background).

Table 2: Random errors expected in the LHC dipoles assuming mechanical tolerances of $50 \mu\text{m}$ cut at 1σ . Unit 10^{-4} at the reference radius $R_{ref} = 17 \text{ mm}$.

	statistical model		extrapolations from Hera		uncertainty	
n	σ_{b_n}	σ_{a_n}	σ_{b_n}	σ_{a_n}	σ_{b_n}	σ_{a_n}
3	0.64	0.65	1.44	0.43	0.87	0.84
4	0.40	0.41	0.49	0.49	0.34	0.49
5	0.24	0.25	0.65	0.33	0.42	0.42
6	0.15	0.15	0.28	0.14	0.57	0.57
7	0.09	0.08	0.25	0.25	-	-
8	0.05	0.05	0.21	0.22	-	-
9	0.03	0.03	0.22	0.29	-	-
10	0.02	0.02	0.24	0.24	-	-
11	0.01	0.01	0.20	0.20	-	-

Table 3: Random multipolar errors calculated from ROXIE assuming mechanical tolerances of $50 \mu\text{m}$ and of $100 \mu\text{m}$ cut at 3σ . Unit 10^{-4} at the reference radius $R_{ref} = 10 \text{ mm}$.

n	50 μm		100 μm	
	σ_{b_n}	σ_{a_n}	σ_{b_n}	σ_{a_n}
3	1.23	1.21	2.42	2.40
4	0.76	0.79	1.49	1.55
5	0.44	0.47	0.85	0.92
6	0.26	0.27	0.51	0.53
7	0.17	0.16	0.31	0.31
8	0.09	0.08	0.18	0.16
9	0.05	0.05	0.09	0.09
10	0.03	0.03	0.05	0.05
11	0.02	0.01	0.03	0.03

3 Errors induced by stresses

Collaring, assembling and thermal stresses induce a non-negligible deformation of the coil conductors in the LHC dipoles. The deformations can be computed by a finite element code like ANSYS [3], and program like ROXIE can be used to evaluate the induced multipolar errors.

We performed this analysis on the LHC dipole with two-in-one and five blocks design, and we computed the magnetic errors at three successive stages during the magnet production, i.e. in the collared coil, in the yoked warm magnet, and finally in the cold magnet at injection.

In Tab. 4 we give the expected variations of the multipolar components at the three stages of interest. In the three situations considered, the expected mechanical deformations are non-negligible in size, consequently they induce a quite substantial variation of the multipolar. In addition, even if the deformed shape is quite different from a situation to an other, the induced multipolar variation is similar in size, at least for the allowed odd harmonics. The even harmonics, instead, vary quite considerably.

This result is qualitatively confirmed by the available magnetic measurements of a few 10 m long prototype dipoles [4]. We are not yet able to predict with precision the absolute value of the measured multipoles due to our imperfect knowledge of the mechanical characteristics of the prototype magnets.

Table 4: Variation of the multipoles expected from coil deformations. Unit 10^{-4} at the reference radius of 17 mm.

	COLLARED	ASSEMB.	COOLED
b_2	+1.62	+2.42	+9.79
b_3	+7.11	+7.00	+6.08
b_4	-0.03	-0.04	-0.21
b_5	-0.77	-0.33	-0.49
b_6	-0.05	+0.04	+0.15
b_7	+0.31	+0.18	+0.15
b_8	-	-	-0.01
b_9	-0.08	+0.03	+0.03
b_{10}	-	+0.06	+0.36
b_{11}	-0.12	-0.06	-

But we see that the allowed harmonics measured at the various stages of dipole completion do not change very much, in agreement with our computer simulations.

4 Shimming as corrective action

A possible way to reduce the field-shape imperfection of a magnet consists in changing the coil geometry by a set of shims selected 'ad hoc' [5]. We investigate this possibility in the LHC dipole using a computer model based on ROXIE.

Our aim is to find the range of tunability of the multipoles and to verify if in this range the dependence on the shim size is still linear.

We assume that shims up to $200 \mu m$ thickness can be inserted in the mid-plane and in the pole of both the inner and the outer coils. We also assume that we can vary the size of the four copper wedges by the same amount. In this range the variation of the multipolar components is linear with the variation of the thickness. In Table 5 we show the change of multipoles due to shims of $100 \mu m$. In the first four cases the shims were added in the inner midplane, inner pole, outer midplane and outer pole respectively, while in the last three cases the shims were added to the wedges between the blocks. In all cases we assumed that the change of the coil geometry is uniform along the azimuth. The shims have a significant effects on

Table 5: Effect of shims on multipolar errors. Note that wed_1 is in the outer layer; wed_2 and wed_3 are in the inner layer. Unit 10^{-4} at the reference radius of 17 mm.

	b_3	b_5	b_7	b_9	b_{11}
i_{mid}	-3.17	-0.88	-0.24	-0.05	-0.03
i_{pol}	+1.90	-0.43	+0.18	-0.10	0.01
o_{mid}	-1.31	-0.19	-0.02	-	-
o_{pol}	+1.49	-0.05	-0.02	-	-
wed_1	-0.38	+0.04	+0.02	-	-
wed_2	-1.53	+0.15	+0.22	+0.10	+0.01
wed_3	+2.41	+0.36	-0.25	-0.02	+0.03

the allowed harmonics at the same time. However one can act on a single harmonics by an appropriate set shims. For a full control of them we may have to introduce the shims already in the nominal coil design in order to make possible positive or negative changes of the block size. To act on even multipolar errors a left-right asymmetric set of shims is to be used. The corresponding variation of the multipolar errors is reported in Table 6. The effect on low order harmonics, like the normal quadrupole and octupole is significant but unfortunately not independent.

Table 6: Effect of left-right asymmetric shims on multipolar errors. Unit 10^{-4} at the reference radius of 17 mm.

	inner coil	outer coil
b_2	+1.80	+2.85
b_3	+0.80	+1.02
b_4	+0.15	-0.22
b_5	-0.04	-0.23
b_6	-0.03	+0.05
b_7	-0.01	+0.10
b_8	-	-
b_9	-	-0.05
b_{10}	-	-0.03
b_{11}	-	-

Although from a practical point of view only the upper pole shims seem to be easily realizable after the building of the coil, an effective control of the lower multipolar errors requires the possibility of using shims also in the midplane.

5 Local Compensation of Random Errors by Dipoles Sorting

In general random fluctuations of the magnetic imperfections due to constructing tolerances affect substantially the stability of the particle motion. Unfortunately it may be very difficult if not impossible to correct each individual magnet. The sorting strategies are considered an appropriate tool to compensate the destabilising effect of the random errors of the superconducting magnets in large hadron colliders [6, 7]. It has been shown that installing at appropriate locations along the accelerator the magnets with large random errors, can provide to a large extent a self compensation of their detrimental effects thereby improving the dynamic aperture.

The techniques proposed for the sorting of the main LHC dipoles are based on local or quasi-local cancellation of the random errors by pairing the magnets with similar errors in magnitude and sign and placing each pair in a strategic position along the azimuth of the accelerator [8, 9, 10]. The strategies developed were first tested on a simplified model of the LHC where only random errors were included in the main dipoles and tracking was performed considering only the short term dynamic aperture (1000 turns) in the 4D motion. The most promising techniques were then applied to a realistic model of the LHC where all multipolar errors were included in the dipoles and the dynamic aperture was computed including the synchrotron motion, power supplies ripple in the main quadrupoles. Long term effects in beam stability were considered by tracking particles up to 10^5 turns and analysing the survival plots by means of the extrapolating laws for the long term estimates of the dynamic aperture [11, 12].

Pairing at zero phase advance. Taking into account that two adjacent dipoles have optical functions not too dissimilar and the phase advance between them is almost negligible, one can obtain a local compensation scheme by placing in adjacent position two errors equal in strength but with opposite signs. Indeed this scheme is used for the correction of the systematic b_3 and b_5 errors in the LHC dipoles by means of spool pieces correctors. In the LHC the scheme is only partially effective since the phase advance between two dipoles is approximately 15 degrees.

Pairing at 180 and 360 degrees. In absence of strong deviation from the linear motion, a better cancellation scheme of equal and opposite random errors can be obtained by placing the magnets at position separated by 360 degrees or equivalently 180 degrees for errors also equal in sign. In the LHC each cell contains 6 dipoles and the phase advance is 90 degrees so that positions separated by 24 magnets correspond to a phase advance of 360 degrees. Furthermore owing to the regularity of the cells, these position correspond to the same location in the cell therefore the optical functions are equal.

Mixed techniques. It is possible to define sorting procedures based on more than one of the previ-

ous strategies. The pairing of two adjacent magnets can be improved by a compensation at 360 or 180 degrees. In this case 4 dipoles are paired.

Further improvement of these technique can be obtained by the minimisation of dynamical quantities such as perturbative estimations of tune shifts or resonance driving terms by means of random permutations of the previously generated pairs of dipoles^[9, 13, 14]. In the following we present the effect of mixed techniques on LHC models of increasing complexity.

5.1 4D Analysis of the LHC motion

We initially applied the sorting algorithms described above to the LHC version 2, with the injection optic, available at that time. The lattice was made of 8 octants, each of them carrying 16 dipoles in the dispersion suppressor region and 144 dipoles in the arcs. Each arc is composed of 24 FODO cells each carrying 6 dipoles. The overall number of dipoles is 1280. The set of 376 chromatic sextupoles is considered in the simulations. We assume that the magnets will be installed as the production goes on, therefore only a limited number of dipoles will be stored and available for sorting. We applied the sorting strategies on groups of 144 dipoles. We also assumed that only random errors are included in the main dipoles and we calculated the dynamic aperture with short term tracking (1000 turns) on 4D motion. Two extreme cases were analysed in detail: dipoles with only random b_3 , and dipoles with the full set of random errors.

We generated 100 random realization of the multipolar errors and calculate the dynamic aperture by tracking before and after sorting the dipoles. The characteristics of the distribution of the DA and the results of the sorting strategies are reported in Table 7. The average value over 100 realizations is denoted by D and the R.M.S. by σ_D . The improvement of the DA due to the sorting of the cases with an initially small value of the DA are denoted as 'Worst Cases' in Table 7. The effect of sorting on the DA can be put in evidence by plotting the relative gain in DA as a function of the DA of the unsorted realizations of the errors, as shown in Figs. 3 and 4. It appears clearly that the realizations with an initially small value of the DA are more efficiently corrected and in the worst cases the DA is more than doubled. The results

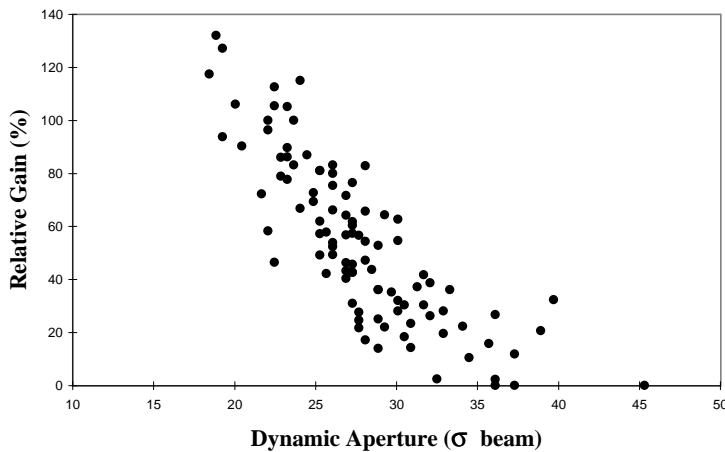


Fig. 3: Relative gain as a function of the DA of the unsorted sequence of random errors for 100 realizations. Only random b_3 .

of these studies show that the sorting strategies we developed are very effective in the case where there is a dominant multipole e.g. the case with only random b_3 . In the general case, where all random errors up to 11-th order were included, the improvement in dynamic aperture, although reduced with respect to the previous simplified case, is still significant at least for the realization of the random errors which have a small dynamic aperture before sorting.

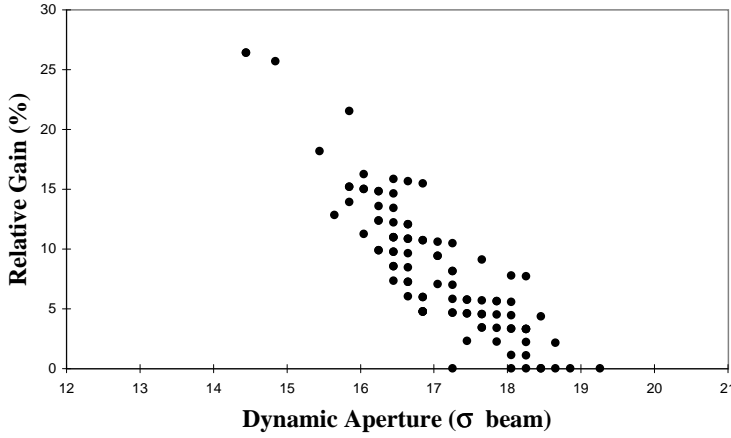


Fig. 4: Relative gain as a function of the DA of the unsorted sequence of random errors for 100 realizations. All random errors.

Table 7: Characteristics of the DA distribution over 100 random realizations of the multipolar errors. 4D motion LHC v2.

	D	σ_D	Gain	Worst Cases
b_3 random errors.				
unsorted	27.8	4.77	-	
sorted	40.9	4.55	48%	91%
Random errors up to 11-th order.				
unsorted	17.0	0.97	-	-
sorted	18.2	0.54	7%	17%

5.2 Long terms and 6D checks

The robustness of the sorting strategies developed was tested on a realistic and more recent model, the LHC version 4.3. Extensive tracking simulations were performed including all multipolar errors in the main dipoles and quadrupoles, both systematic and random, coupling with the longitudinal motion and power supplies ripple in the main quadrupoles. Furthermore a more realistic value of 48 dipoles was assumed to be available from the storage areas. The characteristics of the corresponding DA distribution before sorting are given in Tab. 8. Owing to the large amount of CPU time needed, sorting strategies were applied only to the five worst cases. Although the absolute gain in DA is small, in all cases the value obtained after sorting is close to the average value of the distribution of DA for the unsorted realization which accounts to say that the worst realizations can at least be corrected to average realizations.

The extrapolation of the survival plots allows to estimate the long term behaviour to a number of turns as large as 10^6 . The plots of the DA vs the number of turns N obtained from tracking up to 10^5 turns are interpolated using the empirical formula [12]

$$D(N) = A + \frac{B}{\log^k N} \quad (1)$$

to obtain DA estimates at 10^6 turns.

Table 8: Characteristics of the DA distribution over 30 random realizations of the multipolar errors. 6D motion LHC v4.3.

$D(10^3)$	$\sigma_{D(10^3)}$	$D(10^5)$	$\sigma_{D(10^5)}$
13.36	0.49	11.89	0.49

Table 9: DA values calculated at 10^3 , 10^5 , 10^6 turns for the 5 worst realizations of the random errors before and after sorting.

	D(10^3) tracking	D(10^5) tracking	D(10^6) extrapolation
unsorted			
# 1	12.20	10.37	9.61
# 4	12.35	11.22	10.93
# 9	12.33	11.23	10.81
#19	12.26	10.90	10.35
#29	12.02	10.57	9.71
sorted			
# 1	13.11	11.59	11.02
# 4	13.36	12.08	11.69
# 9	12.91	11.76	11.29
#19	12.74	11.70	11.42
#29	13.23	11.42	10.89

This analysis shows that the gain in DA persists and an example of the comparison of the survival plot for a realization (seed #1) of the random errors is shown in Fig. 5. The values of the DA for these 5 cases, before and after sorting, is given in Table 9.

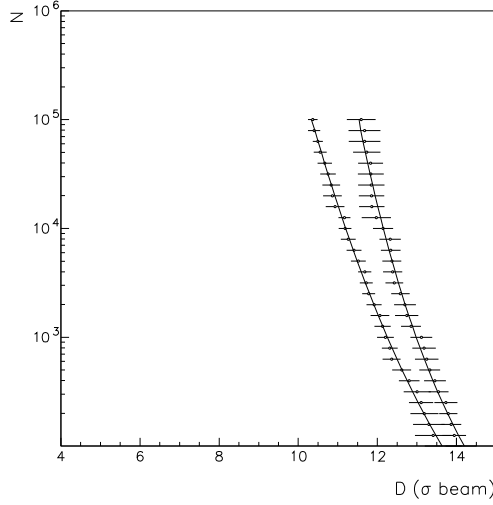


Fig. 5: Interpolation of survival plot for the realization seed #1. The leftmost curve is the survival plot before sorting, the rightmost after sorting.

6 Conclusions

The geometrical coil imperfections of the LHC dipole play an essential role in the determination of random and systematic field-shape imperfections. The numerical analysis of the random multipoles due to the variation of the coils and collars geometry within the allowed tolerances shows that low order multipoles may be more affected by the collar imperfections; instead, high order multipole may be more affected by the positioning errors of the individual blocks. The deformations of the conductors resulting from mechanical and thermal stresses modify significantly the systematic multipoles already present in the nominal design. Methods to reduce the multipoles can be based on the use of set of shims by which one can vary the coil geometry. Shims of one or two hundred of μm size are already adequate for our needs. However, we would like to suggest in the near future slight changes of the collar geometry so

to prevent at least the increase of the systematic field-shape errors. The effect of the random multipolar errors on the dynamic aperture was investigated with extensive tracking studies. Sorting strategies were applied to realistic LHC models and they have shown to be effective in those cases where the dynamic aperture is significantly influenced by the random errors.

REFERENCES

- [1] S. Russenschuck et al., *Europ. Phys. J. Appl. Phys.* **1**, (1998) 93–102.
- [2] R. Perin, private communication, (1996).
- [3] ANSYS 5.4, licensed by and trademark of Swanson Analysis Inc., Houston, PA, USA.
- [4] O. Pagano, L. Bottura, private communication, (1998).
- [5] R. Gupta, in *EPAC 96*, edited by S. Myers, A. Pacheco, R. Pascual, Ch. Petit-Jean-Genaz and J. Poole (Institute of Physics Publishing, Bristol and Philadelphia, 1996) pp. Vol. II, 917-919.
- [6] F. Willeke, *DESY HERA* **87-12** (1987).
- [7] R.L. Gluckstern e S. Ohnuma, IEEE Transactions on Nuclear Science, **NS-32**, (1985), pp. 2314–2316.
- [8] W. Scandale, L. Wang, *CERN SPS (AMS)* **89-22** (1987).
- [9] R. Bartolini, M. Giovannozzi, W. Scandale, E. Todesco in Particle Accelerator Conference, edited by American Physical Society (IEEE, Piscataway, USA, 1997) in press.
- [10] D.M. Ritson, *CERN LHC Project Note* **53** (1996).
- [11] M. Giovannozzi, W. Scandale, E. Todesco, *Part. Accel.* **56**, (1997) 195–225.
- [12] M. Giovannozzi, W. Scandale, E. Todesco, *Phys. Rev. E* **57**, (1998) 3432–3443.
- [13] M. Giovannozzi, R. Grassi, W. Scandale, E. Todesco, *Phys. Rev. E* **52**, (1995) 3093–3101.
- [14] R. Bartolini, M. Giovannozzi, W. Scandale, E. Todesco, *Nuovo Cimento B* **113**, in press and CERN LHC Project Note **38**, (1995).